Acta Oceanol. Sin., 2015, Vol. 34, No. 11, P. 71–79
DOI: 10.1007/s13131-015-0750-4
http://www.hyxb.org.cn
E-mail: hyxbe@263.net

Observational analysis of the double-diffusive convection in the deep Canada Basin

XIE Lingling[1], LI Mingming[1]*, LI Min[1]

[1] Guangdong Province Key Laboratory for Coastal Ocean Variation and Disaster Prediction (GLOD), Guangdong Ocean University, Zhanjiang 524088, China

Received 19 March 2015; accepted 4 July 2015

©The Chinese Society of Oceanography and Springer-Verlag Berlin Heidelberg 2015

Abstract

The Canada Basin (CB) is the largest sub-basin in the Arctic, with the deepest abyssal plain of 3 850 m. The double-diffusive process is the possible passage through which the geothermal energy affects the above isolated deep waters. With the temperature-salinity-pressure observations in 2003, 500-m-thick transition layers and lower 1 000-m-thick bottom homogenous layers were found below 2 400 m in the central deep CB. Staircases with downward-increasing temperature and salinity are prominent in the transition layers, suggesting the double-diffusive convection in deep CB. The interface of the stairs is about 10 m thick with 0.001–0.002°C temperature difference, while the thicknesses of the homogenous layers in the steps decrease upward from about 60 to 20 m. The density ratio in the deep central CB is generally smaller than 2, indicating stronger double-diffusive convection than that in the upper ocean of 200–400 m. The heat flux through the deepest staircases in the deep CB varies between 0.014 and 0.031 W/m^2, which is one-two orders smaller than the upper double-diffusive heat flux, but comparable to the estimates of geothermal heat flux.

Key words: double diffusion, Canada Basin, staircase, heat flux, water mass

Citation: Xie Lingling, Li Mingming, Li Min. 2015. Observational analysis of the double-diffusive convection in the deep Canada Basin. Acta Oceanologica Sinica, 34(11): 71–79, doi: 10.1007/s13131-015-0750-4

1 Introduction

Diapycnal mixing is the critical factor of the oceanic meridional circulation, where differential diffusion of heat and salt plays an important role in both the properties of water masses and global conveyor belt (for instance, Gargett and Ferron, 1996; Munk and Wunsch, 1998). As is recognized, diapycnal mixing in the abyssal ocean is generally formed by two mechanisms: the turbulent mixing induced by breaking of internal waves, or the double diffusion due to the instable vertical structure(s) of temperature and/or salinity in the stably stratified ocean, and the latter one is further classified as salt fingering and double-diffusive convection. Schmitt et al. (2005) suggested that salt fingering intensified the diapycnal mixing, while the thermal and saline diffusivities were both larger than those of turbulent mixing observed in abyssal ocean. The study of double diffusion is thus important to further understanding of oceanic mixing, transportations of heat, mass and momentum, and to the development of numerical models of ocean circulation (Ruddick and Gargett, 2003).

The unique vertical structures of temperature and salinity at high latitudes suggested the presence of double-diffusive processes there. As a matter of fact, the double diffusion in the Arctic Ocean (AO) has been supported by various observations and analyses (Neal et al., 1969; Neshyba et al., 1971; Padman and Dillion, 1987, 1989; Timmermans et al., 2003, 2008; Cao and Zhao, 2011; Zhao and Zhao, 2011; Lique et al., 2014). In 1969, Neal et al. already found strong layering structures suggestive double-diffusive convection in abyssal AO. It was supposed to be the major attribution of the thermocline intrusions in the AO (May and Kelley, 2002), which was responsible for the climate changes of the arctic in recent decades (Carmack et al., 1997, 2012). Moreover, due to the possible effect in the formation of the northern water masses, the double-diffusive convection might be an important factor of the global climate system.

As the largest sub-basin in the AO, the Canada basin (CB) with the deepest abyssal plain of 3 850 m has the largest volume among those in the AO, and possibly contains the oldest deep water. According to the estimation of ^{14}C, deep water in the CB (below 2 200 m) is about 450 years old (Schlosser et al., 1997). This specific basin is laterally separated by the Lomonosov Ridge and the Alpha-Mendeleyev Ridge (MR) from the ocean, further isolated by vertical stratifications, thus direct ventilation is consequently not possible in this area (Macdonald et al., 1993). The variations of the water masses properties in the deep basin were assumed to be the result of abyssal fluxes from bottom (such as geothermal energy), where the double-diffusive processes are the possible passage through which the heat flux affects the above water masses (Timmermans et al., 2003).

Double-diffusive staircase structures have been observed in the upper boundary of the warm Atlantic water in the CB (such as Neal et al., 1969; Padman and Dillion, 1989; Timmermans et al., 2008), with step thicknesses around 1–10 m, temperature differences of 0.004–0.026°C between adjacent layers and vertical heat flux of 0.05–0.30 W/m^2. Zhao and Zhao (2011) analyzed the distribution of double-diffusive staircase structure in the upper CB, and suggested that the striking staircases generally spread

Foundation item: The National Natural Science Foundation of China under contract Nos 41476009, 41106012 and 41506018; the Science and Technology Program in Higher Education of Guangdong under contract No. 2013KJCX0099.
*Corresponding author, E-mail: mingming.li@vip.126.com

through the depth range of 100–500 m over the Mendeleyev Ridge. Nevertheless, double-diffusive processes in the deep basin were seldom studied. In this paper, the double diffusion in the abyssal CB was analyzed using the CTD casts measured during the second Chinese Arctic expedition of R/V *Xue Long* in 2003. The data and method are described in Section 2. The properties of temperature-salinity profiles and θ-S curves are detailed in Section 3, followed in Section 4 by quantifying the strengths of staircase structures induced by double-diffusive convection and the estimations of consequent heat flux. Differences between upper and abyssal double-diffusive structures are compared in Section 5, the results are discussed in Section 6 and Section 7 is the summary.

2 Data

In the second Chinese Arctic Expedition carried out by R/V *Xue Long* during July 23 to September 13 in 2003, temperature (T) and salinity (S) were measured at various stations inner and nearby the CB with MARKIII CTD produced by the Neil Brown Ocean Sensors Incorporated (NBOSI). The resolutions of temperature, salinity and depth are 0.000 5°C, 0.001 and 0.1 m respectively. Two representative sections are analyzed in this study: one is over the Chukchi plateau near the MR (Section M) and the other is in the abyssal central basin (Section B). Locations of these stations are listed by black dots in Fig. 1. The data used here were conventionally processed and averaged into 1-m intervals prior to further processing. Then the potential temperature (θ) were computed referring to 0×10^4 Pa; outliers of θ and S were excluded and then they were movingly smoothed with 3-m interval.

3 Properties of water masses in the Canada Basin

3.1 *Along vertical sections*

As shown in Fig. 2, the potential temperature and salinity profiles at different stations have similar vertical structures. The temperature has uniformly low values in the upper 30 m near sea surface; a sub-surface thin warm layer appears at around 50–100 m, and then the temperature decreases to the minima below –1.5°C at around 150 m; higher temperature is found through 200–1 500 m with the maxima more than 0.6°C at around 400 m, and then decreases again to a minimum of –0.53°C at around 1 800/2 400 m upon the warmer mixed waters near the bottom. The vertical structure of salinity is relatively simple: 0–30 m, the fresh mixed layer; 30–400 m, the halocline where salinity increases significantly with depth, with larger gradient between 30 and 200 m and smaller one through 200–400 m; and increases with little gradient below 400 m till the homogenous waters near the bottom.

The horizontal distributions of the potential temperature and salinity are also clear in Fig. 2. The major meridional variation of temperature concentrates in the shallow layer above 200 m, where it increases from the north to south and the thickness of mixed layer decreases simultaneously, especially to Stas S25 and S24 south of 75°N along Section B. The depth of the warm subsurface layer also varies with locations: it is shallower at Stas M06 and M07 than that in the northern part, companied with shallower warm cores. Comparing to Section M over the Chukchi plateau, the surface mixed layer is thicker for Section B in the central basin, with lower temperature for the warm core at around 400 m depth. Furthermore, cold water is found between 1 800–2 000 m in Section M but much deeper at 2 300–2 500 m in Section B. The salinity is relatively uniformly distributed along these meridional sections, except the change in the surface mixed layer, where the salinity increases from north to south along Section B, but is opposite for Section M. The surface water is also fresher along Section B.

3.2 *θ-S diagram*

The θ-S diagram is remarkably useful in recognition and analysis of water masses. According to the θ-S diagrams shown in Fig. 3 and the previous vertical structures of temperature and salinity in Fig. 2, four distinctive water masses are recognized from top to bottom in the CB: a relatively cold and fresh water above 30 m, with temperature generally lower than –1.0°C and salinity smaller than 29, diluted by surrounding rivers and melting sea ices of Atlantic and Pacific Ocean (Smethie et al., 1999); a subsurface water between 30 and 200 m, located in the halocline with great salinity gradient (0.03 m^{-1}) and characterized by its unique thermal features with temperature maxima at 50–100 m, which is possibly due to the summer inflow through the Bering

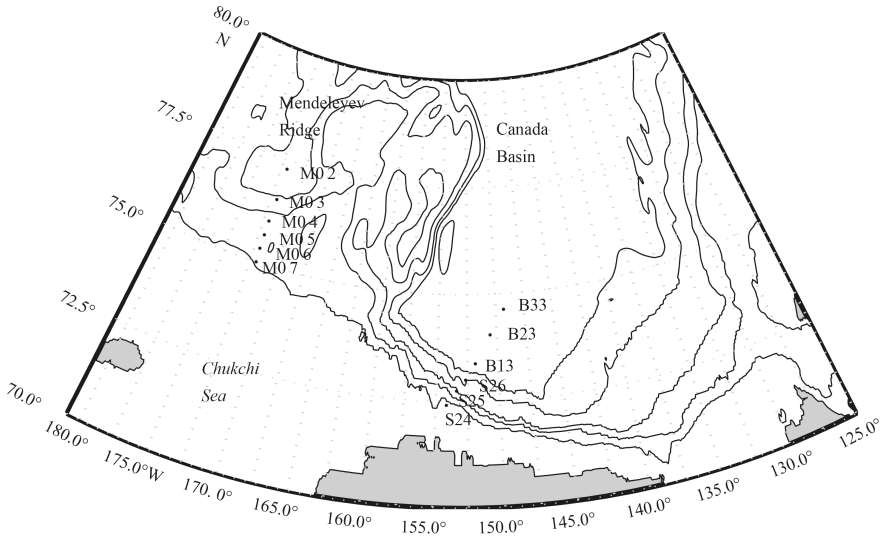

Fig. 1. The topography (contour lines) and station locations (black dots) in the Canada Basin.

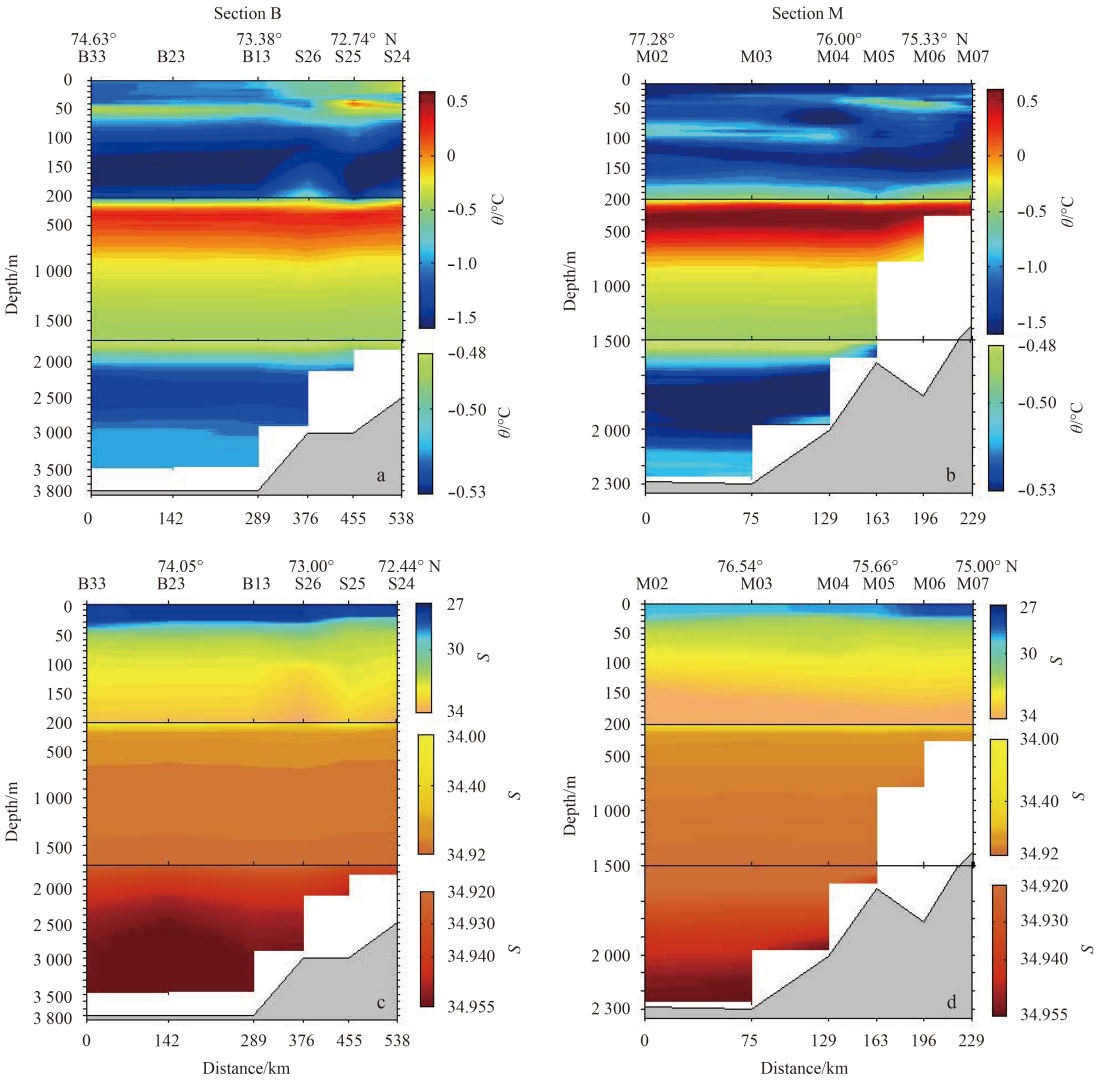

Fig. 2. Vertical structures of potential temperature θ (a, b) and salinity S (c, d) along two Sections B and M.

strait (Aagaard et al., 1981), and the low temperature at 150 m may be the residue of cold core formed in winters (Zhao et al., 2003); a relatively warm saline mid-depth water through 200–1 500 m, also called the Atlantic Intermediate Water, of which the temperature and salinity increase with smaller gradient (0.006 m^{-1} in salinity) within depths of 200–400 m featured as the lower halocline. This mid-depth water is originated from the warm, saline and dense Atlantic water (Aagaard et al., 1985; Carmack et al., 1995). The fourth one is a relatively well-mixed saline deep water, which extends from 1 500 m to the bottom with mean temperature of –0.5°C and salinity around 34.95.

The double-diffusive processes are usually related to the features of large scale water masses. According to profiles along two sections and θ-S diagrams in Fig. 3, temperature and salinity increase simultaneously within 200–400 m. The spreading of cold fresh water over warm saline water suggests the possible existence of double-diffusive convection, as is reported of the staircase structures in this upper layer by former researchers (e.g., Zhao and Zhao, 2011). When focus on the deep layer, we notice an upturn below 1 500 m in the θ-S diagram, where temperature decreases with depth to the minima and then increases again. Alternatively, if we choose 2 000 ×10^4 Pa or 3 000 ×10^4 Pa as the reference level of potential temperature θ, the upturn is still present (not shown in this paper). Zooming in the deep part of θ-S diagram to Fig. 4, we can see that the potential temperature decreases first and then increases with salinity in the bottom water, which indicates the existence of a layer of temperature minima. For Section B in the deep basin, the minima are –0.524–-0.525°C at salinity of 34.951–34.955; for section M over the Chukchi plateau, the minima of θ are –0.535–-0.545°C at salinity of 34.935–34.945. Below the minimum-temperature layer, θ increases with the increase of salinity downward. The vertical structure of such cold fresh water over warm saline water provides the prerequisite of the double-diffusive convection. One can also see the lump dots for Section B, indicating the homogenous temperature and salinity of the mixed layer in the staircases of double diffusion.

4 Features of double-diffusive convection in the deep CB

4.1 *Staircase characteristics*

The double-diffusive processes are generally represented by regular staircase structures of temperature and salinity, that is to say, well mixed layers separated by thin interfaces (Turner, 1968,

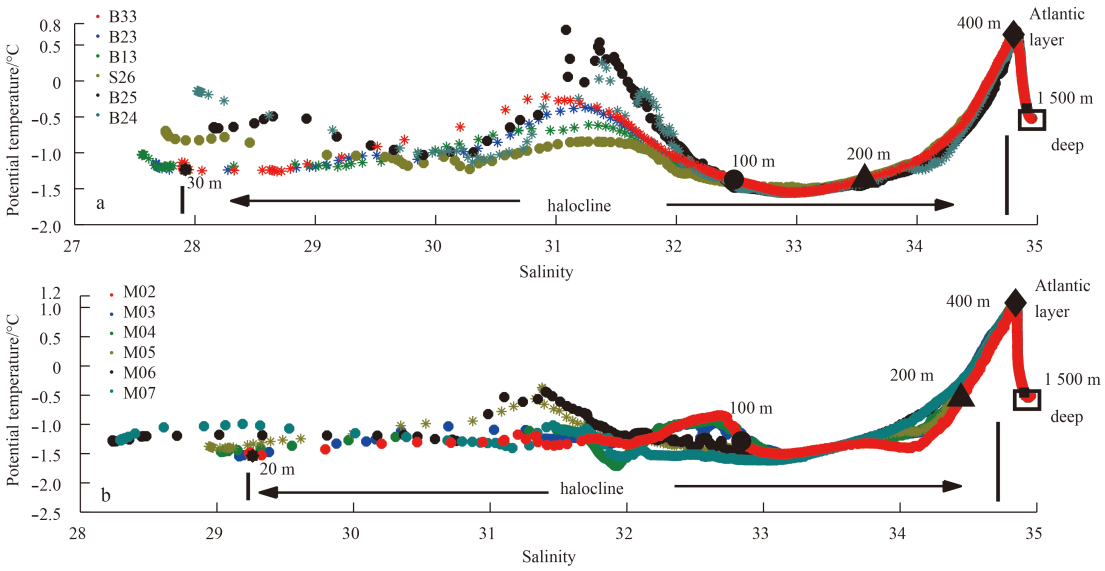

Fig. 3. θ-S diagrams of Sections B (a) and M (b).

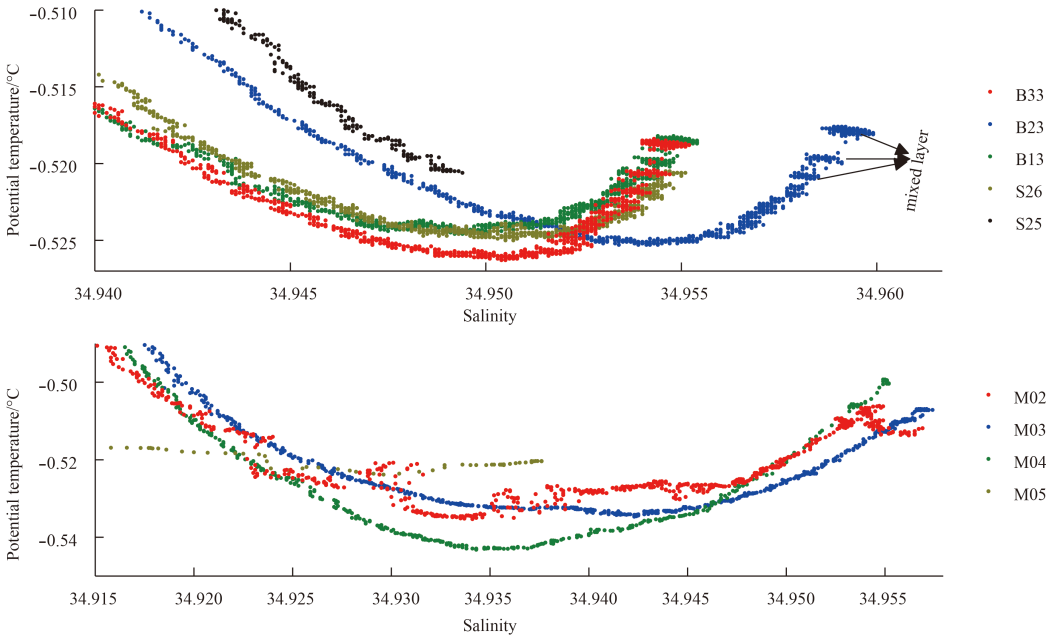

Fig. 4. θ-S diagrams below 1 500 m for deep water, amplified from Fig. 3.

1973). The vertical profiles of θ and S at stations below 1 500 m along the sections are illustrated in Fig. 5. It is shown that along Section M near the MR, potential temperatures reach the minima of –0.535–-0.543°C at 1 800–1 900 m at Stas M02, M03 and M04, and then increase to –0.51°C downward as salinity increasing monotonically with depth. The gradient of salinity at Sta. M04 is apparently larger than those at Stas M02 and M03 in the north. Along Section B in the central basin, the potential temperature reaches its minima of –0.526°C at around 2 450 m (the depth of MR is 2 400 m), increases with depth and reaches its maxima of –0.519°C at around 2 950 m, and remains nearly constant from around 3 000 m to the bottom. The salinity increases monotonically with depth above 2 950 m, and then remains constant of 34.955 to the bottom. The layer where potential temperature increases with depth is named as the transition layer and the layer below 3 000 m with homogeneous θ/S as the bottom mixed layer. The transition layers and bottom mixed layers are widespread in the deep central CB (Timmermans et al., 2003). Here we choose the layers between the depths of θ minima and the top of homogeneous bottom layers as the transition layers, which have an average thickness of around 500 m, and the thickness of homogeneous bottom layer (bottom mixed layer) is up to 1 000 m. Distinct staircase structures of temperature induced by the double-diffusive convection can be found in transition layers, especially at depths close to the bottom layer. However, the bottom mixed layer is not clear along Section M, and the staircase structures there are also weaker than those along Section B.

The detailed structures of the temperature staircases in trans-

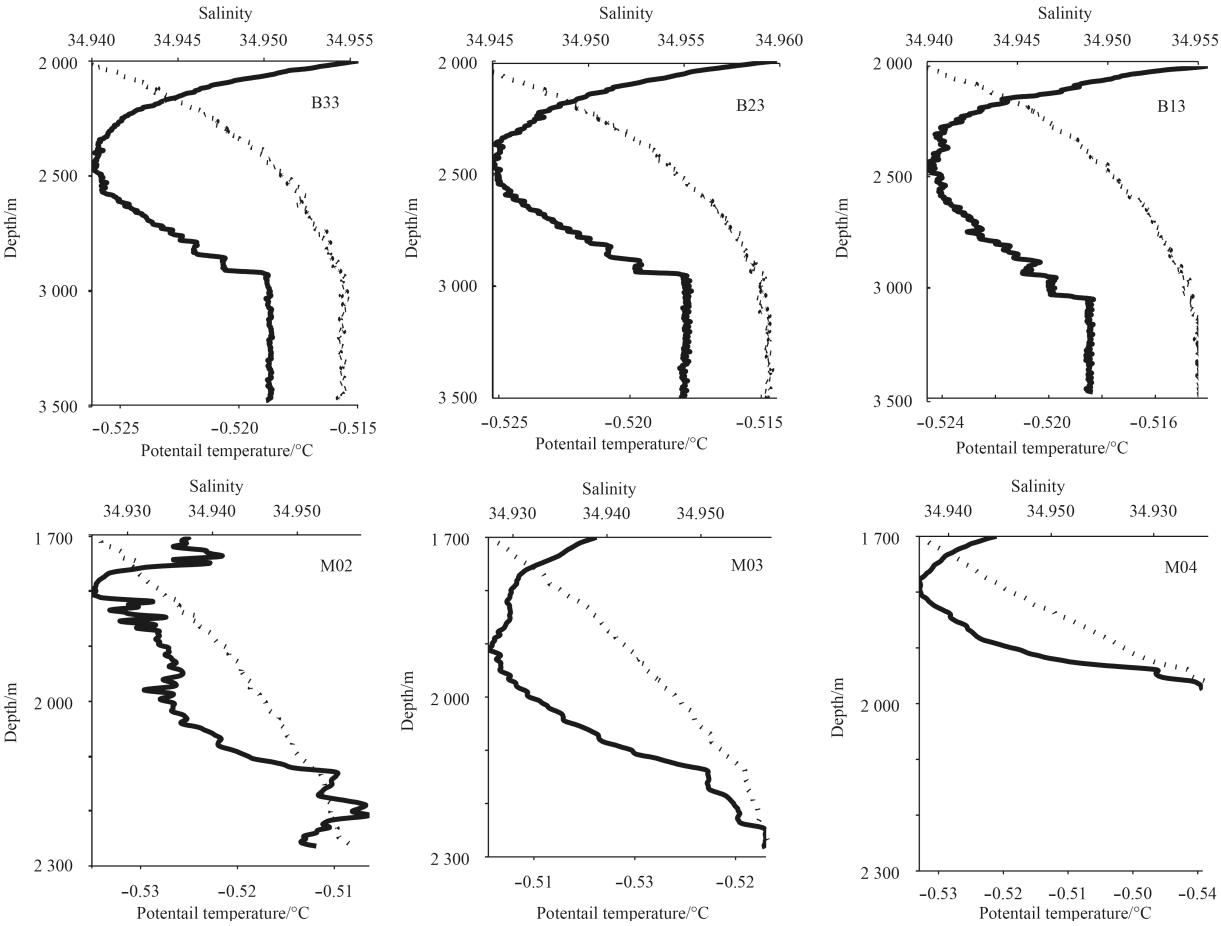

Fig. 5. Profiles of θ and S in the deep layer of Stas B33, B23, and B13 along Section B and Stas M02, M03 and M04 along Section M. Solid lines: potential temperature; dash lines: salinity.

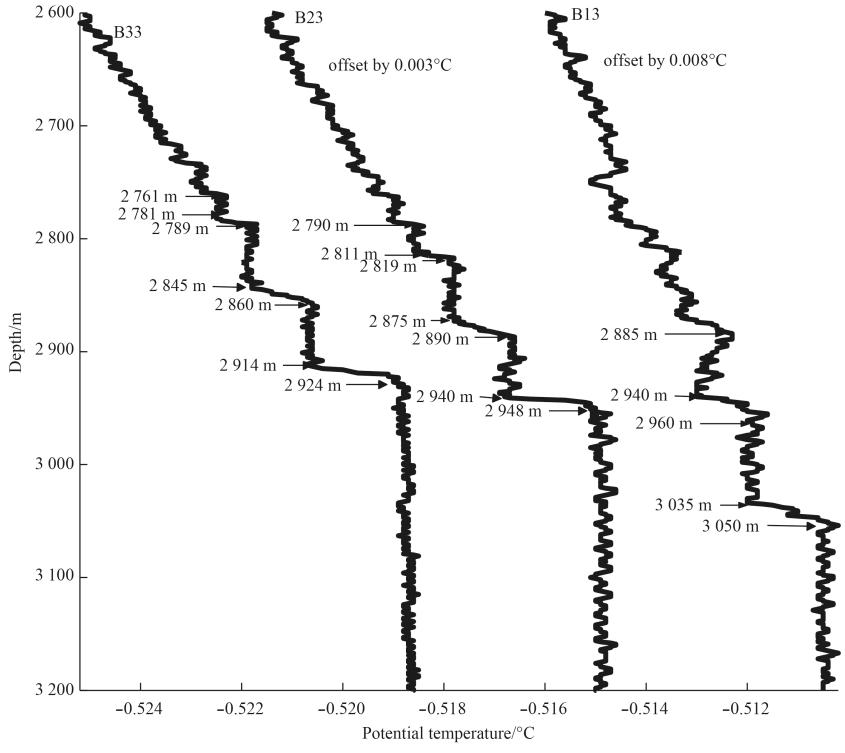

Fig. 6. Deep staircase structures at stations along Section B in the central Canada Basin.

ition layers along Section B are illustrated in Fig. 6. Compared to the double-diffusive staircases over the Chukchi plateau along Section M, those in the deep CB are more regularly shaped, with thicker mixed layer and interfaces but less stairs. Specific to single profile, the staircase structure is most clear near the bottom, and the thickness of mixed layers decreases upward, from around 50 to 20 m, while the thickness of interfaces remains constant of around 10 m. The upper boundary of the bottom mixed layer gets deeper from north (2 924 m at Sta. B33) to south (3 060 m at Sta. B13), and the number of regular steps decreases with the thinning of the bottom mixed layer. The details of the staircase structure are listed in Table 1.

4.2 *Strengths of the double-diffusive convection*

It was suggested by Turner (1973) that the strength of double diffusion could be represented by the density ratio R_ρ (also called the temperature and salinity gradient ratio, or the coefficient of stabilization). For double-diffusive convection, it is defined as $R_\rho = \beta S_z / \alpha\theta_z$, where $\alpha = -\rho^{-1}(\partial\rho/\partial T)$ is the thermal expansion coefficient, $\beta = \rho^{-1}(\partial\rho/\partial S)$ the saline contraction coefficient, and $S_z = \partial S/\partial z$, $\theta_z = \partial\theta/\partial z$ the vertical gradients of salinity and temperature, ρ the density. When $1<R_\rho<10$ the double-diffusive convection offers great potential and when $R_\rho \to 1$ the strength of double-diffusive convection reaches its maximum (Kelley et al., 2003). R_ρ values of deep staircases along Section B are listed in Table 1. The values are in the range of 1.4–2.4 of which most are less than 2 in the deep CB, indicating the considerable probability of strong double-diffusive convection.

4.3 *Heat flux*

Many parameterizations of heat fluxes across double-diffusive interfaces in oceanic situation have been derived from laboratory experiments combined with theoretical analyses, and various formulations lead to similar results (Kelley et al., 2003; Timmermans et al., 2003). Here we use the formulation suggested by Kelley (1990) to estimate the heat flux across double-diffusive interfaces in the CB:

$$F_H = -0.003\,2\mathrm{e}^{\left(4.8/R_\rho^{0.72}\right)}\rho\left(\frac{\alpha g\kappa}{P_r}\right)^{1/3}(\delta\theta)^{4/3}\,, \qquad (1)$$

here P_r=ν/k is the Prandtl number, ν=1.89×10^{-6} m^2/s the kinematic viscosity, k=1.28×10^{-7} m^2/s the thermal diffusivity, and g=9.8 m/s^2.

As is shown in Fig. 6, we choose the interface between the homogeneous bottom layer (of thickness h_0) and the nearest mixed layer (of thickness h_1) as the first interface (of thickness δh_1), and the following interfaces upward as the second and third interfaces. Corresponding heat fluxes of deep double-diffusive convection across these interfaces are indicated by F_{h_n}. As listed in Table 1, the heat fluxes through the deepest interfaces are in order of $O(10^{-2})$ W/m^2, with the maximum value of 0.031 W/m^2 at Sta. B33 in the central basin, consistent with the geothermal heat flux in the CB of 0.04–0.06 (Langseth et al., 1990), and smaller values of 0.014 and 0.016 W/m^2 at Stas B23 and B13 in the southern CB. The heat fluxes seem to decrease in the upward staircases, and the minimum value of 0.003 W/m^2 appears at Sta. B23. The magnitudes of heat flux of each interface are summarized in Table 1.

Table 1. Characteristics of the deep staircase structure induced by double-diffusive convection along Section B

Station	δh_1,h_1/m	δh_2,h_2/m	δh_3,h_3/m	$\delta\theta_1$/°C	$\delta\theta_2$/°C	$\delta\theta_3$/°C	R_{ρ_1}	R_{ρ_2}	R_{ρ_3}	F_{h_1}/W·m^{-2}	F_{h_2}/W·m^{-2}	F_{h_3}/W·m^{-2}
B13	15, 75	20, 55		0.001	0.001		1.72	1.62		0.016	0.019	
B23	8, 50	15, 56	8, 21	0.002	0.001	0.001	1.90	2.30	2.39	0.014	0.006	0.003
B33	10, 54	15, 56	8, 20	0.002	0.001	0.001	1.42	2.17	1.95	0.031	0.009	0.006

Notes: δh_1 is the thickness of the interface between the bottom layer and the first (deepest) mixed layer (of thickness h1), δh_2 and δh_3 are the thicknesses of the following interfaces upward, and h_2, h_3 the thicknesses of the second and third mixed layers respectively; $\delta\theta_n$ the changes of potential temperature of the corresponding interfaces and similarly for the density ratio $R_{\rho n;}$ F_{hn} the heat fluxes transferred through corresponding interfaces, the calculation of which is explained in Section 4.3.

5 Differences between deep and upper double-diffusive convection characteristics

Between 200 and 450 m in the upper basin, temperature and salinity increase monotonically with depth due to the existence of the warm saline Atlantic Intermediate Water, where staircase structures also presents, suggesting the double-diffusive convection (Fig. 7). Along Section M over the Chukchi plateau, we find regular staircase structures of θ and S between 280 and 380 m at Stas M02, M03 and M04 (in the north), weak and irregular staircases at Sta. M05, and these steps disappear at Stas M06 and M07 in the shallow coastal area in the south. For Section B, staircase structure of salinity is not found either inner the deep basin (of water depth larger than 3 500 m) or in the south margin adjacent to the Chukchi Sea, and the temperature profiles show more interleaving structure rather than staircase.

Taking Sta. M03 as an example (Fig. 8), we can see steep regular staircases exist between 270 and 350 m, while stairs are not well-formed below 350 m since temperature reaches its maximum at around 400 m and then decreases with the increase of salinity. The stairs become quite thin in the upper 250–270 m, where the mixed-layer thicknesses are only 1 m, comparable to the instrument resolution. No obvious stairs are found above 250 m. For the layer from 270 to 350 m with striking staircase structure, mixed-layer thicknesses h_n vary between 13 and 22 m, while interface thicknesses between 6 and 11 m. The staircase structures at Stas M02, M04 and M05 are similar to Stas M03, though differences exist in depth, thickness and number of staircases and the sequences of the thicknesses. No stairs are found at Stas M06 and M07 close to the Chukchi Sea. The detailed quantitative properties of the staircases at each station are estimated and shown in Table 2.

Comparing the double-diffusive convections in the upper and deep layers, we find that the mixed layer of staircases in the deep CB is about 2–3 times thicker, the density ratios are 1 value smaller, and the heat fluxes are 1–2 orders weaker. The mechanic mixing may enhance the mixed layer of the staircases in the deep CB as the density ratio there are generally smaller than 2 (Timmer-

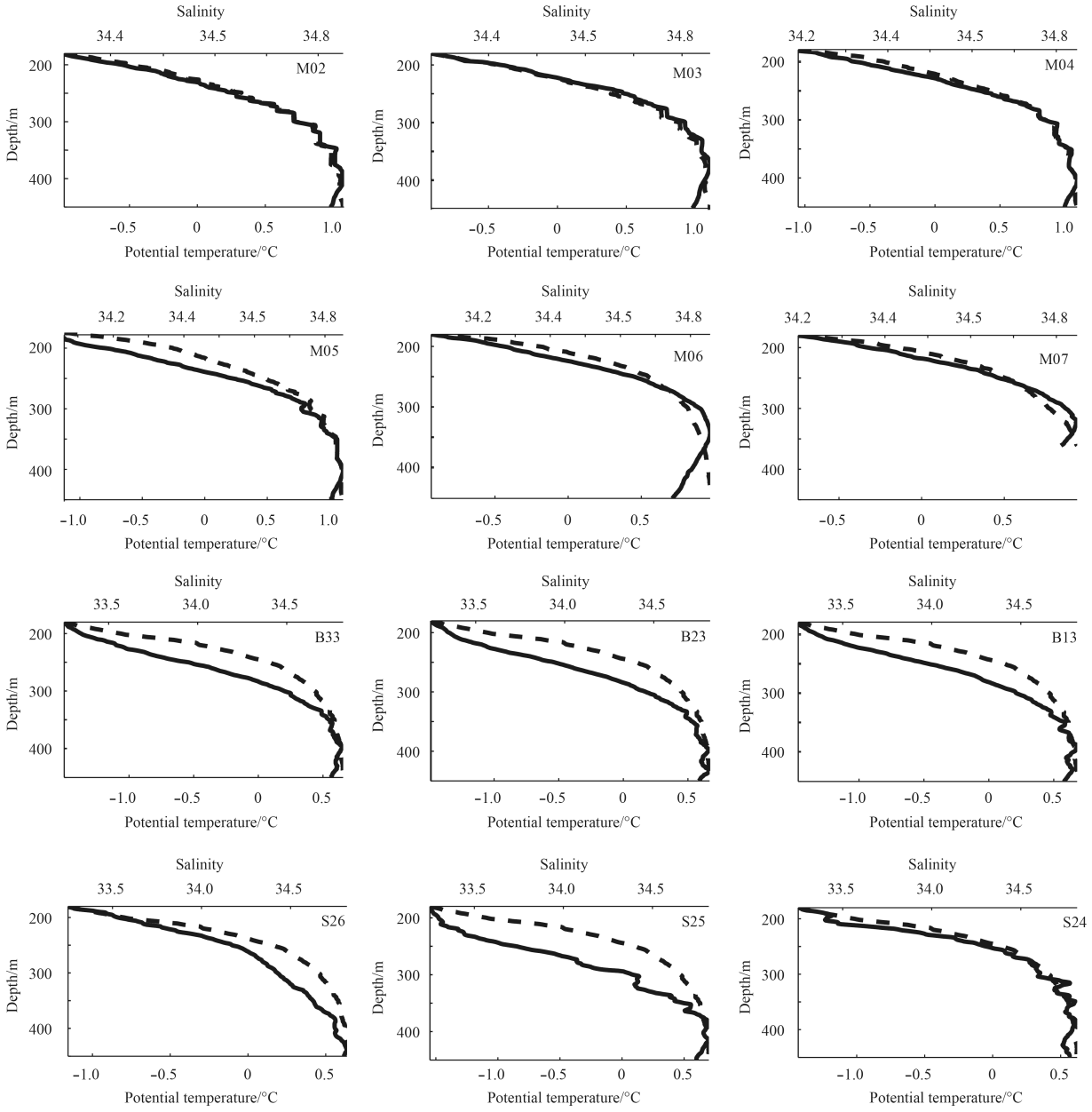

Fig. 7. Staircase structures of temperature and salinity in upper layer. Solid lines: potential temperature; dash lines: salinity.

mans et al., 2003), while the density ratios in the upper ocean is mostly over 3.

6 Discussion

The double-diffusive convection in the upper CB has been focused by previous studies (e.g., Padman and Dillon, 1989). Recently, based on the CTD data of the third Chinese Arctic Expedition in 2008, Zhao and Zhao (2011) found striking double-diffusive staircases with interface thickness of 1–5 m at 300–400 m depth over the MR, and no obvious staircases were found in the southern part of the central basin, while double-diffusive staircases were found at 200–300 m depth in the northern part of the basin by Timmermans et al. (2008). The presence of staircases in the upper layer over the MR and the absence of staircases in the southern CB in this study based on MarkIII CTD data are consistent with Zhao and Zhao (2011)'s results using SBE911 Plus CTD.

In the deep CB, due to the upward diffusion of geothermal heat, the decreasing temperature turns to increase downward below the depth reaching minima as the downward increasing salinity, offering a primary mechanism of the existence of the double-diffusive convection. Most observations in the CB were not deep enough due to technical reasons (especially in early expeditions), less extensive focus was stressed in the deep basin compared to the upper layer. Nevertheless, striking staircase structures were observed below 2 400 m for the θ with measurements of high-resolution CTD instruments in case studies, such as the work of Timmermans et al. (2003), based on combined observations of Guildline 8705, SeaBird (SBE) 911 CTD, Falmouth Sci. Inst. (FSI) ICTD and SBE 25. The thicknesses of interfaces and mixed layers were found varying around 2–16 m and 10–60 m respectively.

This work further shows the staircase structure of θ in the

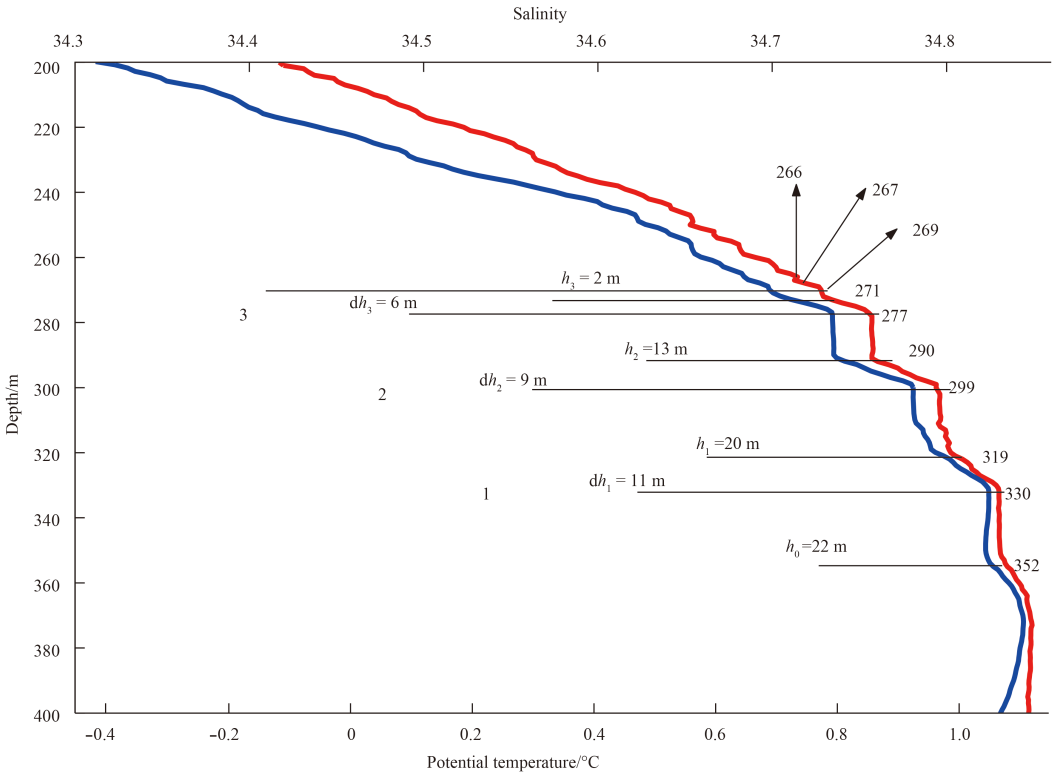

Fig. 8. Staircase structure of θ and S in the upper layer of Sta. M03. The selection of interfaces and transition layers is also demonstrated. Blue line is potential temperature and red line is the salinity.

Table 2. Characteristics of the upper staircase structure induced by double-diffusive convection along Section M

Station	$\delta h_1, h_1$/m	$\delta h_2, h_2$/m	$\delta h_3, h_3$/m	δ_1/°C	δ_2/°C	δ_3/°C	R_{ρ_1}	R_{ρ_2}	R_{ρ_3}	F_{h_1}/W·m^{-2}	F_{h_2}/W·m^{-2}	F_{h_3}/W·m^{-2}
M02	8, 20	4, 9	7, 16	0.107	0.038	0.148	2.17	1.79	2.74	1.89	0.72	1.88
M03	11, 20	9, 13	6, 2	0.090	0.127	0.097	3.18	3.10	3.13	0.77	1.26	0.85
M04	8, 36	7, 16	7, 3	0.075	0.108	0.093	2.77	3.17	3.18	0.75	0.98	0.79
M05	18, 13	10, 14		0.100	0.124		2.85	2.76		1.05	1.47	

Notes: Parameters are similar to Table 1.

deep transition layer of the CB using MARKIII CTD. The salinity difference of the entire transition layer is so subtle (around 0.01 through 500–1 000 m depth) that no salinity staircases is detected, possibly due to the poor resolution of salinity (0.001) by MARKIII CTD. On the other hand, despite the temperature difference in the deep basin is slight (0.005–0.010°C) compared to the upper layer, the high resolution of MARKIII CTD for temperature (0.000 5°C) ensures us to distinguish regular staircase structure of potential temperature. Moreover, the staircases are detected at all abyssal stations in the central basin, precluding the possibility of false manifestation due to technical reasons. Comparing to the observations mainly in early 1990s by Timmermanns et al. (2003), the deep double-diffusive staircase structure and maximal heat flux in the CB in our observation in 2003 show little change. The limited resolutions of the probes might not give the heat fluxes precisely, nevertheless the characteristics of double-diffusive staircases in the deep basin are robust. Further research will be carried out with measurements of following Arctic expedition cruises to investigate the influence of double-diffusive convection on the transformation of deep water masses more accurate.

7 Summary

Based on the CTD measurements in 2003, the staircase structures of temperature and salinity in the deep Canada Basin, suggestive double-diffusive convection, are analyzed in this work. The corresponding magnitudes of the double-diffusive convection are estimated in terms of density ratio R_ρ, and heat fluxes through interface layers of each step are also calculated.

Below 2 400 m in the central basin, 500-m-thick transition layers characterized by monotonic increases of temperature and salinity with depth are found over the bottom homogeneous layer, which are about 1 000 m thick. In the marginal area near the MR, the bottom homogenous layer is much thinner and totally disappears in regions shallower than 2 300 m. Inner the transition layer in the central CB, staircase structures of temperature are induced by the double-diffusive convection, with the interfaces of stairs of around 10 m thick, temperature differences of 0.001–0.002°C for each interface and mixed layers of stairs thinning upward from about 60 m to 20 m.

The density ratio of the staircases in the deep central basin is around 2, 1 value smaller than that in upper layer near MR, where the staircases are thinner, with much larger temperature

gradients across interfaces. The estimation of heat fluxes through the deepest interfaces in the deep basin varies around tens of milliwatt per square meter, and is about two magnitudes smaller than those in the upper marginal area. The maximal heat flux through the deep transition layer is 0.031 W/m^2 in the central basin, comparable to the geothermal heat flux estimations. This work affords strong support to the assumption that the vertical transport of heat across the top of bottom homogeneous layer are mainly carried out by the double-diffusive convection driven by geothermal heat.

Acknowledgements

The authors would like to thank Zhao Jinping and the team of physical oceanography for their special efforts on the fine-structure data collection in the 2nd Chinese National Arctic Research Expedition in 2003. Thanks are also given to two anonymous reviewers for their constructive suggestions.

References

Aagaard K, Coachman L K, Carmack E. 1981. On the halocline of the Arctic Ocean. Deep-Sea Research Part A: Oceanographic Research Papers, 28(6): 529–545

Aagaard K, Swift J H, Carmack E C. 1985. Thermohaline circulation in the Arctic Mediterranean seas. Journal of Geophysical Research, 90(C3): 4833–4846

Cao Yong, Zhao Jinping. 2011. Study on the fine structure of near surface temperature maximum in the Canada Basin in 2008. Haiyang Xuebao (in Chinese), 33(2): 12–19

Carmack E C, Aagaard K, Swift J H, et al. 1997. Changes in temperature and tracer distributions within the Arctic Ocean: Results from the 1994 Arctic Ocean section. Deep-Sea Research Part II: Topical Studies in Oceanography, 44(8): 1487–1502

Carmack E C, Macdonald R W, Perkin R G, et al., 1995. Evidence for warming of Atlantic water in the southern Canadian Basin of the Arctic Ocean: Results from the Larsen-93 Expedition. Geophysical Research Letters, 22(9): 1061–1064

Carmack E C, Williams W J, Zimmermann S L, et al. 2012. The Arctic Ocean warms from below. Geophysical Research Letter, 39: L07604

Gargett A E, Ferron B. 1996. The effects of differential vertical diffusion of T and S in a box model of thermohaline circulation. Journal of Marine Research, 54(5): 827–866

Kelley D E. 1990. Fluxes through diffusive staircases: a newformulation. Journal of Geophysical Research, 95(C3): 3365–3371

Kelley D E, Fernando H J S, Gargett A E, et al. 2003. The diffusive regime of double-diffusive convection. Progress in Oceanography, 56(3–4): 461–481

Langseth M G, Lachenbruch A H, Marshall B V. 1990. Geothermal observations in the Arctic region. In: Grantz A, Johnson L, Sweeney J F, eds. The Geology of North America, The Arctic Ocean Region. Boulder, CO: Geological Society of America, 133–151

Lique C, Guthrie J D, Steele M, et al. 2014. Diffusive vertical heat flux in the Canada Basin of the Arctic Ocean inferred from moored instruments. Journal of Geophysical Research: Oceans, 119(1): 496–508

Macdonald R W, Carmack E C, Wallace D W R. 1993. Tritium and radiocarbon dating of Canada basin deep waters. Science, 259(5091): 103–104

May B D, Kelley D E. 2002. Contrasting the interleaving in two baroclinic ocean fronts. Dynamics of Atmospheres and Oceans, 36(1–3): 23–42

Munk W, Wunsch C. 1998. Abyssal recipes II: energetics of tidal and wind mixing. Deep-Sea Research Part I: Oceanographic Research Papers, 45(12): 1977–2010

Neal V T, Neshyba S, Denner W. 1969. Thermal stratification in the Arctic Ocean. Science, 166(3903): 373–374

Neshyba S, Neal V T, Denner W. 1971. Temperature and conductivity measurements under Ice Island T-3. Journal of Geophysical Research, 76: 8107–8120

Padman L, Dillon T M. 1987. Vertical heat fluxes through the Beaufort Sea Thermohaline staircase. Journal of Geophysical Research, 92(C10): 10799–10806

Padman L, Dillon T M. 1989. Thermal microstructure and internal waves in the Canada Basin diffusive staircase. Deep-Sea Research Part A: Oceanographic Research Papers, 36(4): 531–542

Ruddick B, Gargett A E. 2003. Oceanic double-infusion: Introduction. Progress in Oceanography, 56(3–4): 381–393

Schlosser P, Kromer B, Ekwurzel B, et al. 1997. The first trans-Arctic 14C section: comparison of the mean ages of the deep waters in the Eurasian and Canadian basins of the Arctic Ocean. Nuclear Instruments and Methods in Physics Research Section B: Beam Interactions with Materials and Atoms, 123(1–4): 431–437

Schmitt R W, Ledwell J, Montgomery E, et al. 2005. Enhanced diapycnal mixing by salt fingers in the thermocline of the tropical Atlantic. Science, 308(5722): 685–688

Smethie W M, Schlosser P, Bönisch G, et al. 1999. Renewal and circulation of intermediate waters in the Canadian Basin observed on the SCICEX 96 cruise. Journal of Geophysical Research: Oceans, 105(C1): 1105–1121

Timmermans M L, Garrett C, Carmack E. 2003. The thermohaline structure and evolution of the deep waters in the Canada Basin, Arctic Ocean. Deep-Sea Research Part I: Oceanographic Research Papers, 50(10–11): 1305–1321

Timmermans M L, Toole J, Krishfield R, et al. 2008. Ice-tethered profiler observations of the double-diffusive staircase in the Canada Basin thermocline. Journal of Geophysical Research, 113: C00A02

Turner J S. 1968. The influence of molecular diffusivity on turbulent entrainment across a density interface. Journal of Fluid Mechanics, 33(4): 639–656

Turner J S. 1973. Buoyancy Effects in Fluids. Cambridge: Cambridge University Press

Zhao Jinping, Shi Jiuxin, Jiao Yutian. 2003. Temperature and salinity structures in summer marginal ice zone of arctic ocean and an analytical study on their thermodynamics. Oceanologia Et Limnologia Sinica (in Chinese), 34(14): 375–387

Zhao Qian, Zhao Jinping. 2011. Distribution of double-diffusive staircase structure and heat flux in the Canadian Basin. Advances in Earth Science (in Chinese), 26(2): 193–201